Effective Charges of Polyelectrolytes in a Salt-Free Solution Based on Counterion Chemical Potential

Tzu-Yu Wang,[†] Tzong-Ru Lee,[†] Yu-Jane Sheng,[‡] and Heng-Kwong Tsao*,[†]

Department of Chemical and Materials Engineering, National Central University, Jhongli, Taiwan 320, R.O.C., and Department of Chemical Engineering, National Taiwan University, Taipei, Taiwan, 106, R.O.C.

Received: July 28, 2005; In Final Form: October 3, 2005

The phenomenon of counterion condensation around a flexible polyelectrolyte chain with N monomers is investigated by Monte Carlo simulations in terms of the degree of ionization α, which is proportional to the effective charge. It is operationally defined as the ratio of observed to intrinsic counterion concentration, $\alpha = c_o/c_i$. The observed counterion concentration in the dilute polyelectrolyte solution is equivalent to an electrolyte solution of concentration c_o with the same counterion chemical potential. It can be determined directly by thermodynamic experiments such as ion-selective electrode. With the polyelectrolyte fixed at the center of the spherical Wigner−Seitz cell, the polymer conformation, counterion distribution, and chemical potential can be obtained. Our simulation shows that the degree of ionization rises as the polymer concentration decreases. This behavior is opposite to that calculated from the infinitely long charged rod model, which is often used to study counterion condensation. Moreover, we find that, for a specified line charge density, α decreases with an increment in chain length and chain flexibility. In fact, the degree of ionization is found to decline with increasing polymer fractal dimension, which can be tuned by varying bending modulus and solvent quality. Those results can be qualitatively explained by a simple model of two-phase approximation.

I. Introduction

Charged polymers comprise a broad and interesting class of materials which are very important for biological systems, such as nucleic acids and peptides. However, a salt-free flexible polyelectrolyte solution remains one of the physical systems that are most difficult to understand,[1−6] owing to the long-range nature of the electrostatic interactions and their interplay with the conformation of the charged polymer. Counterions are not distributed evenly in the solution but prefer to stay in the vicinity of the oppositely charged polymers. The extent of counterions residing near the polymer mediates how polyelectrolytes interact among themselves and thus influence the physical properties of polyelectrolyte solutions.

At strong electrostatic coupling, counterions are accumulated close to the surface of the charged particle with intrinsic charge Z. The decorated object (charged particle plus counterions) may be considered a single entity which possesses an effective charge Z^*. The degree of ionization is then defined as $\alpha = Z^*/Z$. The intrinsic charge (in absolute value) can be much greater than the effective charge, $Z \gg Z^*$. The determination of the effective charge varies with the experimental approach.[7−10] It is often considered an adjustable parameter in a fit of experimental data with approximated models. For example, one can infer the effective charge from voltammetry or electrophoresis.

For a structureless macroion, the degree of ionization is a consequence of the competition between the electrostatic internal energy and the counterion entropy. The latter is proportional to $k_BT \ln V$, where V denotes the available volume. For an infinitely dilute solution, i.e., an isolated charged particle, the entropy diverges logarithmically because $V \to \infty$. To confine all counterions, the electrostatic internal energy has to diverge more rapidly than the logarithmic growth. Since the electric potential grows linearly with the size of the charged plane with size L ($\psi_s \sim -L$), the infinitely extended plate possesses infinite surface potential and is able to bind any counterions. On the contrary, the potential energy of a counterion on the surface of a totally ionized sphere with diameter L is finite, $\psi_s \sim -Z/L$. Therefore, an isolated sphere is unable to bind a counterion at finite temperature. In the intermediate case of a rodlike particle, the electric potential diverges logarithmically with the length of the rod ($\psi_s \sim -\ln L$). In other words, the electrostatic energy gain is able to balance the counterion entropy loss for an infinitely extended line. Manning[11] and Oosawa[12] therefore pointed out that the effective line charge density of a rodlike polyelectrolyte is limited to a maximum value determined by this balance point of energy and entropy. All other counterions are "condensed" to the polyelectrolyte.

Unlike structureless charged particles, the polyelectrolyte may undergo conformation change, i.e., from stretching to collapse,[2] when counterions are localized in close proximity to the polyelectrolytes. The change of conformational entropy depends on the chain length as well. For an *isolated* polyelectrolyte with finite length, the aforementioned facts indicate that the polyelectrolyte is unable to bind any counterion, just like a charged sphere. Nonetheless, the counterion entropy, $\sim k_BT \ln c$, is finite in all practical salt-free polyelectrolyte solutions due to finite counterion concentration c. Thus, one expects that charge renormalization takes place eventually when the electrostatic energy gain overwhelms the counterion entropy loss. Evidently, the effective charge associated with a polyelectrolyte in a dilute solution may be affected by many physical factors, including the counterion valency z_c, the line charge density λ, the polymer concentration c_p, the stiffness κ, the solvent quality, the chain length N, and the concentration of the added salt c_s.

* E-mail address: hktsao@cc.ncu.edu.tw.
[†] National Central University.
[‡] National Taiwan University.

10.1021/jp054194m CCC: $30.25
Published on Web 11/05/2005

The conformation properties of a flexible polyelectrolyte in a good solvent have been studied by molecular dynamics. Below a critical value of Coulomb interaction strengths, Winkler et al.[2] observe that the radius of gyration (or end-to-end distance) rises with increasing interaction strength. Beyond the critical value, the polyelectrolyte collapses into a dense coil, because counterions condense on the chain and the formation of ion pairs (dipoles) leads to a net attraction. Using Langevin dynamics simulations and the self-consistent theory based on adsorption mechanism, Muthukumar et al.[4,13] have systematically investigated the distribution of counterions around a flexible polyelectrolyte as a function of z_c, N, c_s, chain flexibility, and $1/\epsilon_r T$ (ϵ_r and T are the dielectric constant of the solvent and temperature, respectively). Their results show that the essential features of counterion condensation for a flexible polyelectrolyte are qualitatively different than the Manning theory for an infinitely long, rigid polyelectrolyte. Although the degree of ionization is found to be independent of N at essentially all Coulomb strengths by Muthukumar et al., α is reported to decline with increasing chain length by Winkler et al. for a given Coulomb strength.

In theoretical studies, the effective charge (degree of ionization) can be determined according to various definitions.[14] The simple and intuitive definition is the two-state approximation, i.e., condensed and free counterions. The boundary between the two states is chosen arbitrarily. For example, the counterions are regarded as being in the condensed state if they are located within a cutoff distance (say, 1.5 counterion diameter) perpendicular to the chain backbone.[2,4] Those counterions neutralize an equivalent number of charges on the polyelectrolyte. The effective charge is therefore the rest of the charge carried by the polymer. Nevertheless, such a two-state definition of the degree of ionization does not relate to thermodynamic quantities.

Another approach to charge renormalization is the electric field felt by a counterion away from the parent macroion.[15] That is, owing to strong screening, the far-field behavior of a highly charged macroion Z is explained by the one associated with a weakly charged macroion Z^*. The nonlinear Poisson−Boltzmann (PB) mean-field description of the counterion clouds is often employed to calculate the electric field. Far from the highly charged macroion, the thermal energy k_BT dominates over the electrostatic potential ψ, and thus, the linearized approximation of the PB theory, yielding the well-known Debye−Hückel (DH) form, is adequate. Assuming that the full PB theory is able to depict the electric field associated with a highly charged macroion, the effective charge can be determined by matching the DH form to the long distance behavior of the "exact" PB solution. The effective charge based on such a definition can also be determined experimentally by the effective interaction potential between two macroions. For example, the DLVO theory,[16] named after Derjaguin, Landau, Verwey, and Overbeek, was adopted to obtain Z^* for spherical colloids.

Since a macroion solution, involving many charged macroions and small ions, is a very complicated system, the Wigner−Seitz (WS) cell is commonly adopted to study the physical properties associated with macroions.[7,11,14,15,17−19] The cell model approximation reduces the theoretical description of the whole system to just one cell. While the interactions among macroions are neglected, the interaction between small ions with their "parent" macroion as well as with small ions is explicitly accounted for in the same cell. Consequently, the cell model approach can be considered an approximate attempt to factorize the partition function in the macroion coordinates, and hence, the many-macroion problem is replaced by a single-macroion problem.[20] The symmetry of the cell may reduce the problem further to a one-dimensional one and allows an analytical treatment.[9] The radius of a spherical WS cell, R, can be related to the concentration of macroions, c_p, by $R = (4\pi c_p/3)^{-1/3}$.

In this paper, we investigate the charge renormalization of a dilute, salt-free polyelectrolyte solution by Monte Carlo simulations in the WS cell. To provide the effective charge with proper thermodynamic meaning, the charge renormalization is performed on the basis of the counterion chemical potential. This definition enables a direct comparison with equilibrium experimental results pertinent to polymer charge. The influences of polyelectrolyte concentration and properties such as chain length, bending rigidity, solvent quality, and line charge density on the degree of ionization are examined. The simulation results are compared to those calculated from the infinitely long charged rod model and qualitatively explained by a simple model based on two-phase approximation.

II. Simulation Details

A. Method. The Monte Carlo (MC) simulations are performed to study the dilute polyelectrolyte solutions based on the Wigner−Seitz cell model. The total volume of the isotropic solution is divided into equal spherical cells; each of those contains a single polyelectrolyte with its counterions. The polyelectrolyte was modeled as a freely jointed chain of N hard spheres of diameter d. The interactions between the bonded beads are through the infinitely deep square-well potentials[21]

$$U_{i,i+1} = \begin{cases} \infty & r < d \\ 0 & \sigma \le r < \zeta d \\ \infty & r \ge \zeta d \end{cases} \tag{1}$$

where $\zeta = 1.4$. Bond crossing (phantom chain) can be prevented by such a choice. There are N_p ($N_p \le N$) regularly spaced, charged monomers, each with point fundamental charge of $-e$. The line charge density is defined as $\lambda = N_p e/Nd$. The middle monomer is fixed in the center of the spherical cell of radius R,[22] which is related to the polymer concentration c_p. The counterion is also modeled as a hard sphere of diameter d with point electric charge of $+e$. The electroneutrality condition requires that $N_p = N_c$. Here, N_c is the number of counterions in the cell. The athermally good solvent is simply represented by a continuous medium of uniform dielectric constant ϵ_r ($\sim$80 for water). The electrostatic interactions among the charged beads and counterions are taken to be the Coulomb energy

$$U_{el}(r_{ij}) = \begin{cases} \dfrac{z_i z_j e^2}{4\pi\epsilon_r\epsilon_0 r_{ij}} & r_{ij} \ge d \\ \infty & r_{ij} < d \end{cases} \tag{2}$$

where ϵ_0 is the permittivity of vacuum, r_{ij} the distance between the charged particles i and j, and $z_i = \pm 1$.

A brief description of the MC simulations is given below. The simulation details can be seen elsewhere.[23] The MC simulations are performed with the traditional Metropolis algorithm in a canonical ensemble. While the middle monomer of the polyelectrolyte is fixed in the center of the cell, the other monomers and the small ions are allowed to move in the cell. Note that in the cell model the interaction between species belonging to different cells is ignored. The diameter of the counterion is assumed to be $d = 0.4$ nm and taken as the unit for the spatial length. At 298 K, the dimensionless energy parameter is given as $e^2/(4\pi\epsilon_r\epsilon_0)k_BTd = l_B/d = 1.785$ for water, where $l_B = e^2/4\pi\epsilon_r\epsilon_0 k_B T \simeq 7.2$ Å is the Bjerrum length. The

moves employed in our simulations were bead displacement motions.[23] Bead displacement moves involve randomly picking a monomer or counterion and displacing it to a new position in the vicinity of the old position. The new configurations resulting from the moves were accepted according to the standard Metropolis acceptance criterion, $P_{acc} = \min[1, \exp(-\Delta U_{el}/k_BT)]$, where ΔU_{el} is the change in the total electrostatic energy of the system due to the move. The system was equilibrated for about 10^5 MC steps per particle, and the production period for each simulation was 5×10^5 steps per particle.

B. Counterion Chemical Potential. The degree of ionization or the effective charge associated with a polyelectrolyte varies with its definition. However, to make comparisons between theoretical and experimental work, one has to adopt definitions based on the thermodynamic or transport properties. In this paper, the definition corresponding to the thermodynamic measurements, i.e., bulk (free) counterion concentration, c, is employed. This can be experimentally determined by the osmometry or ion-selective electrode. The latter reads the counterion concentration of a salt-free polyelectrolyte solution directly on the basis of chemical potential.

In the spherical cell model, the chemical potential associated with counterions is related to the counterion concentration on the surface of the WS sphere with radius R, $c(R)$. Within the cell, the chemical potential is constant everywhere and given by[14,23]

$$\mu = \mu_0 + k_BT \ln c(r)d^3 + \mu_{ex}(r) \tag{3}$$

where μ_{ex} denotes the excess chemical potential. For convenience, the reference chemical potential is set to zero, $\mu_0 = 0$. The ideal (counterion concentration) and excess chemical potentials vary with the radial position and can be evaluated from MC. We divide the spherical volume into 30 spherical shells and record the number of counterions in each shell. The excess chemical potential is obtained by the Widom's method,[14,24] which is the reversible work needed to add a counterion to the system

$$\mu_{ex} = -k_BT \ln\langle \exp(-\Delta U/k_BT)\rangle \tag{4}$$

Figure 1 shows typical distributions of ideal chemical potential $\ln cd^3$, excess chemical potential $\beta\mu_{ex}$, and total chemical potential $\beta\mu$. The counterion concentration $c(r)$ declines rapidly from the particle surface to the boundary of the WS cell because of the attraction of the charged polymer. On the other hand, the excess chemical potential increases from $r = d$ and approaches zero at $r = R$ because of repulsion among counterions. The sum of $\ln c(r)d^3$ and $\beta\mu_{ex}(r)$ yields the total chemical potential, which is essentially constant as illustrated in Figure 1. Thus, the chemical potential can also be calculated by

$$\mu \cong k_BT \ln c(R) \tag{5}$$

III. Results and Discussion

Counterion condensation around a flexible polyelectrolyte in a dilute, salt-free solution is investigated. With the polyelectrolyte fixed in the center of the spherical WS cell, Monte Carlo simulations have been performed to calculate the conformation properties and the distribution of counterions. The effective charge (degree of ionization) will be thermodynamically defined later on the basis of chemical potential. In terms of the degree of ionization, the effects of polymer concentration, line charge density, bending modulus, solvent quality, and chain length on counterion condensation can then be determined.

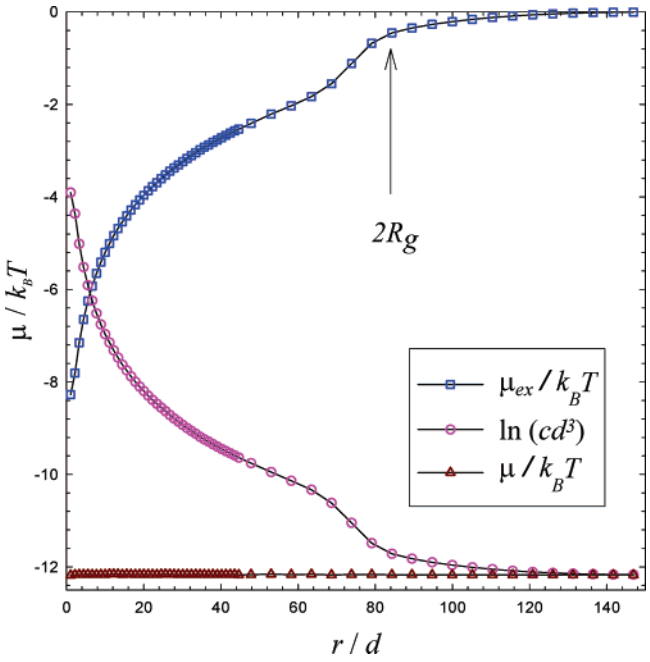

Figure 1. Typical variation of ideal chemical potential ($\ln cd^3$), excess chemical potential (μ_{ex}), and total chemical potential (μ) with the radial distance for $N = 180$, $\lambda = 2.50$ e/nm, and $R = 150d$.

A. Counterion and Monomer Distributions. For a charged sphere or a charged rod, the counterion distribution can be easily used to demonstrate the effective charge or degree of ionization. Owing to the irregular conformation associated with a polyelectrolyte, however, one is unable to define the counterion and charged monomer distributions straightforwardly. The radial distribution functions for counterions g_{cc} and for pairs of monomer and counterions g_{mc} have been employed.[4] Because of the spherical symmetry in our cell model, the counterion and monomer distributions can be orientation-averaged. Whatever the polyelectrolyte conformation is, one can obtain the radial distributions of charged monomers $\rho(r)$ and counterions $c(r)$. Note again that the middle monomer of the polyelectrolyte is fixed in the center of the cell. Figure 2 shows the variation of monomer and counterion with the radial distance for $N = N_p = 180$ and $R = 150d$. When $r < 2R_g$, the monomer charge density is greater than the counterion concentration. Here, R_g represents the average radius of gyration, $R_g^2 = \Sigma_i\langle \mathbf{r}_i^2\rangle/N$, where $\mathbf{r}_i$ is the distance of the bead i from the center-of-mass of the chain and angle brackets denote the averaging over chain configurations. On the contrary, as $r > 2R_g$, the monomer density vanishes rapidly and the counterion concentration decays gradually. This consequence clearly demonstrates that, within the range of the polyelectrolyte chain ($2R_g$), the highly charged polymer is unable to bind all counterions even though the line charge density (about e/4 Å) exceeds the critical charge density (e/7.2 Å) according to the Manning theory. It is because the length of the polyelectrolyte is finite.

The radial distribution of monomers is closely related to the fractal dimension d_f associated with the polyelectrolyte. That is, $\rho(r) \sim r^{-(3-d_f)}$ if the monomers are uniformly distributed along the polymer backbone with fractal dimension d_f. For example, a porous sphere ($d_f = 3$) with uniform space charge density σ has $\rho(r) = (\sigma 4\pi r^2\, dr)/(4\pi r^2\, dr) \sim r^0$, and a rod ($d_f = 1$) with uniform line charge density σ possesses $\rho(r) = (2\sigma\, dr)/(4\pi r^2\, dr) \sim r^{-2}$. Figure 3a,b shows that the radial distributions of both monomer and counterion do follow the power law, $r^{-\alpha}$,

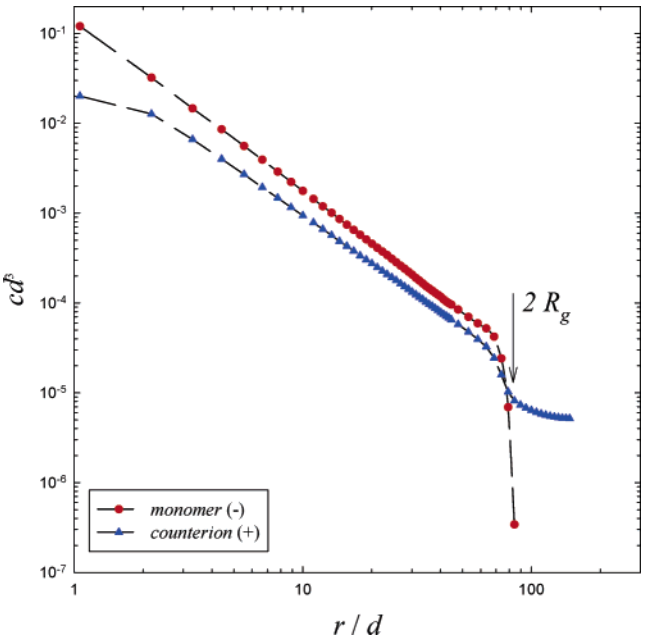

Figure 2. Typical variation of the monomer and counterion concentrations with the radial distance for $N = 180$, $\lambda = 2.50$ e/nm, and $R = 150d$.

for various chain lengths with $N_p = N$. However, the exponents are $\alpha = 1.85$ and 1.67 for monomer and counterion, respectively. This result indicates that the charged polymer has a fractal dimension $d_f = 1.15$, which resembles a straight line. Similarly, if the counterion cloud is regarded as a fractal object, one also has $c(r) \sim r^{-(3-d_f)}$. Figure 3b illustrates that the shape of the counterions surrounding the polyelectrolyte displays the fractal dimension $d_f = 1.33$. In other words, the shape of the polyelectrolyte is more stringy than that of the counterion cloud. If all counterions condense on the polyelectrolyte, one should has the same exponents for both $\rho(r)$ and $c(r)$. However, the expansion of the counterion cloud reveals that the counterion entropy perturbs the electrostatic attraction.

B. Degree of Ionization. *1. Operational Definition.* In a dilute, salt-free polyelectrolyte solution, the counterion concentration would be $\langle c \rangle = c_p N_p / z_c = N_p / [z_c (4\pi R^3/3)]$ if all counterions are released from the polyelectrolyte. However, the electrostatic attractions lead to some counterions "binding" to the polyelectrolyte and result in nonuniform counterion distribution around the charged polymer. It is therefore difficult to define the free counterion concentration simply on the basis of the counterion concentration at an arbitrary position. On the contrary, the thermodynamic properties such as chemical potential of counterions and osmotic pressure are uniform everywhere in the polyelectrolyte solution. Hence, those thermodynamic quantities are ideal for defining the free counterion concentration. The experimental measurement of counterion concentration by ion-selective electrode is based on the principle that the chemical potential of counterions in the polyelectrolyte solution, μ^*, is equivalent to the salt solution of concentration c_b with the same chemical potential of counterions, i.e., $\mu^* = \mu(c_b)$. The free counterion concentration of the polyelectrolyte solution is then defined by c_b, and the degree of ionization is given by $\alpha = c_b / \langle c \rangle$.

In a dilute 1:1 electrolyte solution of concentration c_b, the chemical potential of an ion follows the ideal form, $\mu = \mu_0 + k_B T \ln c_b$, where μ_0 is conveniently set to zero. In the spherical WS cell model, the chemical potential is related to the counterion concentration on the cell surface, $c(R)$, because $\mu_{ex}(R) \rightarrow 0$ as

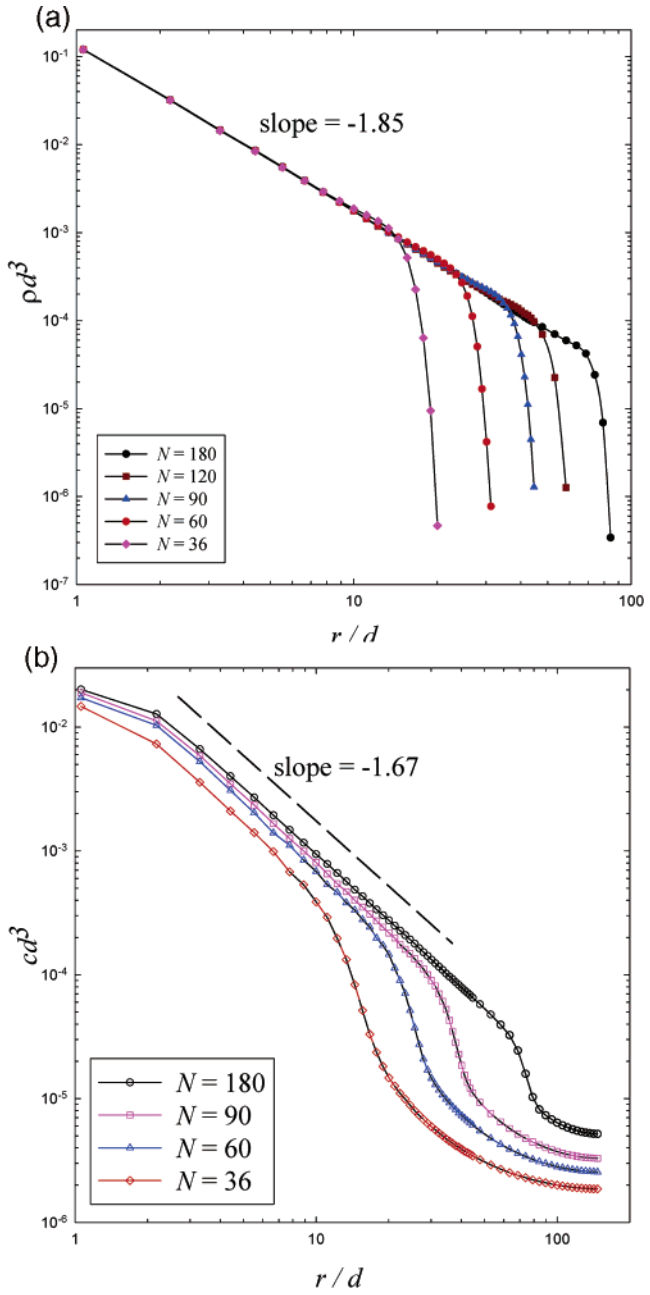

Figure 3. Radial distributions of (a) monomer $\rho(r)$ and (b) counterion $c(r)$ for various chain lengths N at $R = 150d$.

shown in eq 5. As a consequence, the free counterion concentration in the polyelectrolyte solution based on the counterion chemical potential is simply given by $c(R)$. The degree of ionization can then be obtained by

$$\alpha = \frac{c(R)}{\langle c \rangle} \tag{6}$$

The effective charge associated with the charged polymer is therefore obtained as $N_p \alpha$.

2. Infinitely Long Charged Rod and Manning Condensation. The phenomenon of counterion condensation phenomenon has been extensively studied for a salt-free solution of rigid polyelectrolytes on the basis of the nonlinear Poisson−Boltzmann theory.[11,12,19,20,26] In the classic model, an infinitely long, charged cylindrical polyion of radius r_0 and all of its counterions are confined within a cylindrical cell of radius R_c. The exact solution is available[20,26] and indicates that the counterions cannot

be localized for $\xi = \lambda l_B/e < 1$ in the limit of infinite dilution. However, the charged rod with $\xi > 1$ is able to condense a fraction of $1 - \xi^{-1}$ of all counterions even when $R_c \rightarrow \infty$. Such counterion condensation, referred to as "Manning condensation", reduces (renormalizes) the effective line charge density to $\lambda = e/l_B$, and the rest of counterions remain not localized. According to the definition of the degree of ionization in eq 6, α for strongly charged polyions is given by

$$\alpha \cong \frac{1}{2\xi} \quad \text{for } \xi > 1 \tag{7}$$

For weakly charged polymers, the degree of ionization can be evaluated as

$$\alpha \cong 1 - \frac{\xi}{2} \quad \text{for } \xi \leq 1 \tag{8}$$

Note that $R_c \rightarrow \infty$ (infinite dilution) for both regimes. The above results indicate that the crossover of α from linear decrease to λ^{-1} decay signifies the onset of Manning condensation.

C. Line Charge Density λ. For the present model polyelectrolyte, the charged monomers are regularly spaced and the line charge density can be defined as the charges per unit length along the polymer backbone or $\lambda = N_p e/Nd$. The maximum line charge density is one fundamental charge per bead. It is anticipated that the conformation varies significantly with the line charge density because of electrostatic contributions. In terms of the exponent associated with radius of gyration, $R_g \propto N^{\nu}$, ν is altered with λ for a given chain length N. Figure 4a shows the variation of the structure factor $S(q)$ with qR_g for $N = 96$. Here, $\mathbf{q}$ represents the wave vector. For $qR_g \gg 1$, one has asymptotic behavior, $S(q) \propto (qR_g)^{-1/\nu}$. Therefore, the exponent $\nu(\lambda)$ can be estimated from Figure 4a. As the linear charge density is increased, the exponent rises from $\nu \simeq 0.6$ to $\nu \simeq 0.9$. That is, the charged polymer changes from a random coil to a stringlike structure. Because of the increment of ν, the radius of gyration is also increased with λ for a given chain length, as shown in Figure 4b. On the basis of the blob picture, the conformation of the polyelectrolyte is regarded as an extended assembly of electrostatic blobs, within which the electrostatic energy is balanced by the thermal energy. With increasing λ, the blob size ($\sim\lambda^{-6/7}$) declines, but the number of electrostatic blobs grows more rapidly. The size of the polyelectrolyte is thus increased with the line charge density, and $R_g \sim \lambda^{4/7}$ for a rodlike configuration.[27] In Figure 4b, the polymer size can be approximated by $R_g \sim \lambda^{0.64}$ for a given chain length despite of the fact that the electrostatic blob picture may be invalid for such short chains.

The concept of persistent length l_p, which represents a measure of stiffness or correlation along the chain, is useful in describing the conformational characteristics of polyelectrolyte solutions. In the present study, the uncharged polymer ($\lambda = 0$) is intrinsically flexible, and its persistent length is $l_p \simeq 2d$. Since electrostatic repulsions among charged monomers tend to elongate the polymer, the persistent length l_p is expected to grow with increasing line charge density. There are a few definitions of persistent length.[28] To be closely related to the experimental persistent length, we adopt the project length that denotes the projection of the end-to-end vector ($\mathbf{R}_e$) on the direction of the first bond ($\mathbf{r}_2 - \mathbf{r}_1$)

$$l_p = \left\langle \frac{\mathbf{r}_2 - \mathbf{r}_1}{|\mathbf{r}_2 - \mathbf{r}_1|} \cdot \mathbf{R}_e \right\rangle \tag{9}$$

For a given chain length at $R = 150d$, Figure 4c shows that the persistent length increases slowly at small $\lambda(e/3d)$ but grows very rapidly at large λ. It can be realized by the comparison between the spacing between charges e/λ and the Bjerrum length $l_B = e^2/4\pi\epsilon_r\epsilon_0 k_B T \simeq 7.2$ Å. Note that, in a dilute, salt-free polyelectrolyte solution, the Debye screening length is large or comparable to the size of the chain, and hence, the electrostatic interactions are essentially unscreened. In the system we studied, the Debye screening length κ^{-1} is greater than about $60d$. Consequently, the dependence of the persistent length on the screening length is insignificant. When $e/l_B\lambda < 1$, the electrostatic repulsion between the neighboring charged monomers dominates over the thermal energy and tends to stretch the chain. The long-range nature of the unscreened Coulomb interaction enhances the polymer elongation furthermore. On the contrary, as $e/l_B\lambda < 1$, the thermal energy wins for a finite chain length. Our results are qualitatively consistent with the classical OSF theory,[32,33] $l_p \propto \lambda^2$, as will be shown in eq 15 later.

When the line charge density is increased, the degree of ionization is expected to decline, as illustrated in Figure 5 for $R = 150d$, because of the electrostatic energy gain. However, two different features between flexible polyelectrolyte and charged rod are observed. First, the characteristic of linear decrease in weakly charged regime and algebraic decay in strongly charged regime, as depicted by the Manning theory for charged rods, is absent for flexible polyelectrolytes. The transition at $l_B\lambda/e = 1$ signifies the onset of counterion condensation for rigid polyions. Second, the degree of ionization is less than that of a rigid polyelectrolyte ($N \rightarrow \infty$ and $R_c \rightarrow \infty$) and varies with the chain length N at the same line charge density. Note that a polyelectrolyte with finite chain length is unable to localize counterions at infinite dilution.

D. Polymer Concentration c_p (WS cell radius R). The effect of the polyelectrolyte concentration on α is manifested through the WS cell radius R. Evidently, the available space for the translation entropy of counterions grows with decreasing polyelectrolyte concentration. As a consequence, the degree of ionization declines with increasing c_p for given line charge density and chain length. Figure 6 shows the variation of α with R for $N = 60$ and $l_B\lambda/e = 2.5$. One can see that $\alpha \rightarrow 1$ as $R \rightarrow \infty$. That is, in infinitely dilute limit, the entropy gain dominates over the electrostatic energy loss and all counterions are completely free. A comparison between our simulation results and the Poisson−Boltzmann theory based on the rigid rod model may reveal the applicability of the latter in dilute, flexible polyelectrolyte solutions.

In the rigid rod model,[20,26] the polyelectrolyte is infinitely long, and the polymer concentration c_p is related to the cylindrical radius R_c by $c_p = (\pi R_c^2)^{-1}$. Opposite to the results for flexible polyelectrolytes, the degree of ionization actually declines with increasing radius of the cylindrical cell, as shown in the inset of Figure 6. In the asymptotic limit, $R_c/r_0 \gg 1$, one has the analytical expressions

$$\alpha(R_c) \cong \left(1 - \frac{\xi}{2}\right) + \left(\frac{1-\xi}{\xi}\right)\left(\frac{r_0}{R_c}\right)^{2(1-\xi)} \quad \text{for } \xi \leq 1 \tag{10}$$

and

$$\alpha(R_c) \cong \frac{1 + \left[\dfrac{\pi}{\ln(R_c/r_0)}\right]^2}{2\xi} \quad \text{for } \xi > 1 \tag{11}$$

Although the variation of the degree of ionization with the cell

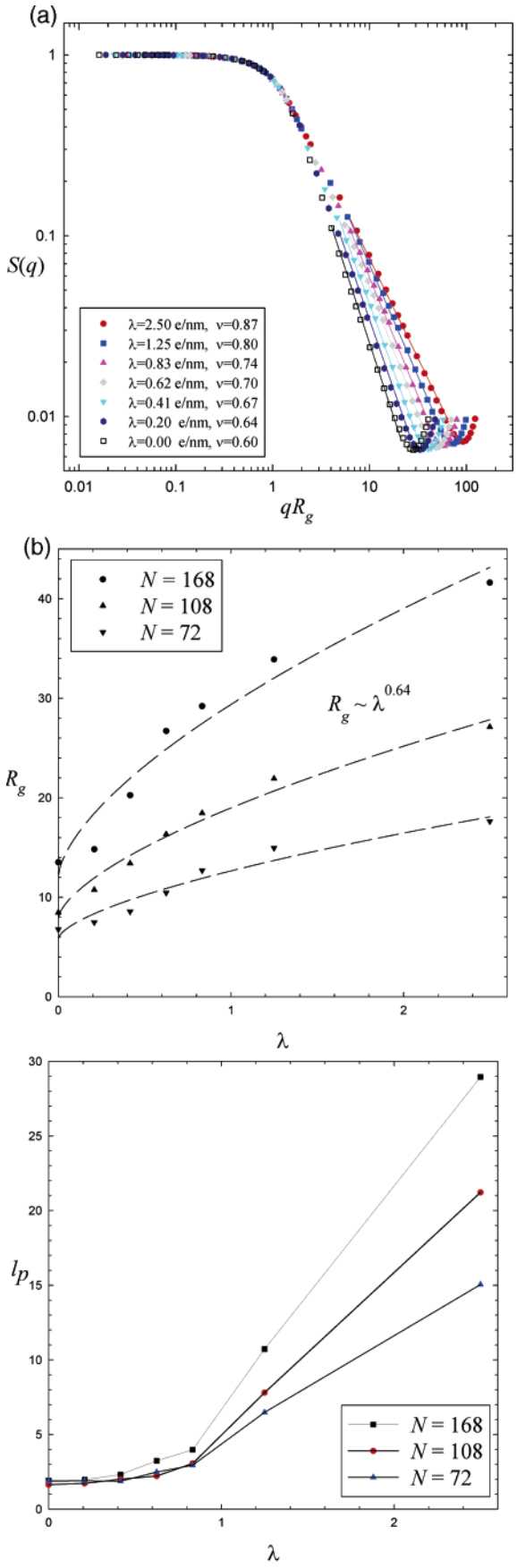

Figure 4. (a) Variation of the static structure factor with qR_g for various line charge densities at $N = 96$. (b) Variation of the radius of gyration with the line charge density for various chain lengths. (c) Variation of the persistent length with the line charge density for various chain lengths.

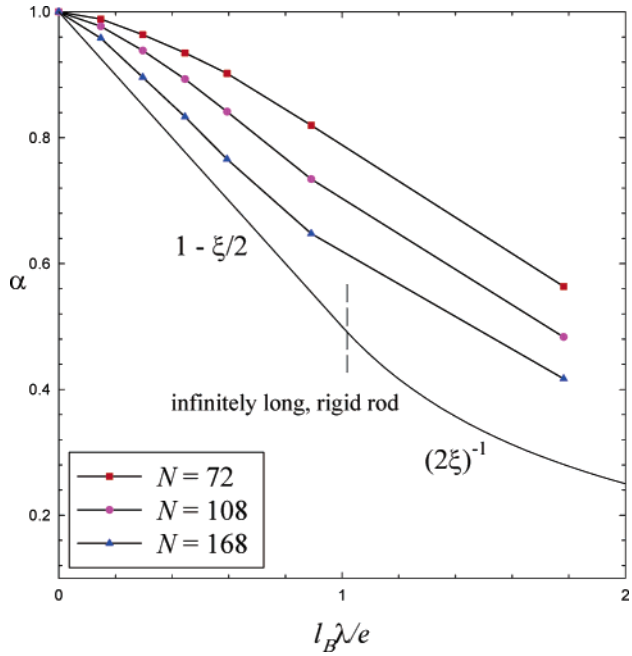

Figure 5. Variation of the degree of ionization with the dimensionless line charge density $l_B\lambda/e$ for various chain lengths.

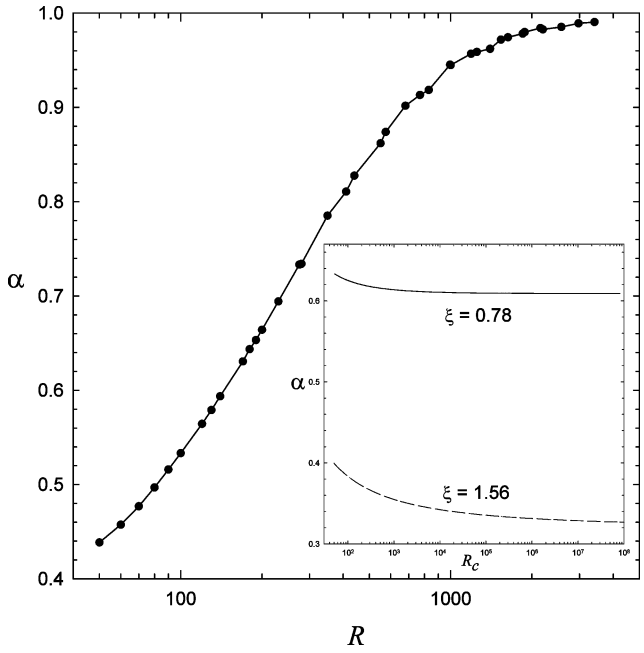

Figure 6. Variation of the degree of ionization with the WS cell radius (polymer concentration) for $N = 60$ and $\lambda = 2.50$ e/nm. In the inset, the degree of ionization for the infinitely long charged rod model is plotted against the cylindrical cell radius for different dimensionless line charge density.

radius is insignificant as $R_c \gg r_0$, this consequence unmistakably shows the opposite trend to our results for flexible polyelectrolytes with finite length.

Rubinstein et al.[26,29] have pointed out that the rigid rod model represents the situation in semidilute and concentrated solutions where the distacne between chains is smaller than the chain size. To generalize the Manning theory of counterion condensation to the dilute solution of rigid polyelectrolytes with finite length, they present a two-zone model.[26,29] Similarly to our WS cell model, each charged rod is placed at the center of a spherical cell of size R. The cell volume $V = c_p^{-1}$ is further divided into two zones: a cylindrical zone (surrounding a rodlike polyion)

with radius R_c on the order of the size of each polyion) and a spherical zone (outside the cylindrical zone). If the degree of ionization is approximated by the osmotic coefficient ($\phi = \Pi/\langle c\rangle k_B T$, where Π is the solution osmotic pressure), one has[29]

$$\alpha = \frac{V}{V_c}\frac{(1-\xi_c)^2 - \xi_c{}^2 - \gamma^2}{2\xi} \tag{12}$$

where γ is determined by R_c, ξ, and ξ_c

$$\left(\frac{R_c}{r_0}\right)^{2\gamma} = \left[\frac{(\xi - 1 - \gamma)(\xi_c - 1 + \gamma)}{(\xi - 1 + \gamma)(\xi_c - 1 - \gamma)}\right] \tag{13}$$

Here, V_c and ξ_c denote the volume and the reduced, effective line charge density associated with the cylindrical zone. The case of electroneutral cell $\xi_c = 0$ ($V_c = V$) reduces to the infinitely long rigid rod model for "semidilute" solutions. Equation 12 indicates that the degree of ionization declines with increasing polyelectrolyte concentration for a given R_c. This trend is consistent with our result depicted in Figure 6.

E. Bending Rigidity βk and Solvent Quality $\beta\epsilon$. So far, MC simulations are performed for intrinsically flexible polyelectrolytes. That is, the monomers interact with each other only with excluded-volume interaction in addition to the Coulomb repulsions. The interactions between monomers may actually consist of the bending rigidity and van der Waals attraction. To systematically explore the effect of polyelectrolyte conformation on the degree of ionization, we alter the bending rigidity and solvent quality but maintain the electrostatic interaction the same.

The stiffness of a wormlike chain is controlled by the bending energy, which can be represented by[30,31]

$$U_b = \sum_{i=2}^{N} k(\mathbf{u}_i - \mathbf{u}_{i-1})^2$$

where $\mathbf{u}_i$ denotes the unit bond vector and k the bending modulus. When $k = 0$, an intrinsically flexible polyelectrolyte is recovered. The persistent length of a charged polymer can be altered by line charge density λ and bending rigidity k. For a given λ, the flexible polyelectrolyte becomes more rodlike with increasing k. According to the analysis of static structure factor, one has $\nu \rightarrow 1$ as $\beta k \rightarrow 20$. Consequently, the polymer exhibits a rigid rod conformation for large enough bending rigidity. Figure 7a illustrates the variation of the degree of ionization with the bending modulus for $N = 60$, $\lambda = 2.5$ e/nm, and $R = 150d$. The fact that α grows with increasing βk and reaches a constant indicates that the extent of counterion condensation is more significant for a flexible polyelectrolyte than for a rodlike polymer ($d_f \rightarrow 1$). The former possesses a smaller characteristic size than the latter and thus is able to result in a stronger electrostatic attraction between counterion and polyelectrolyte.

By varying the solvent quality, we are able to obtain various polymer conformations from the rodlike polyelectrolyte ($d_f \rightarrow 1$) to the compact polymer structure ($d_f \rightarrow 3$). For simplicity, we adopt the square-well potential to depict the monomer−monomer attractions

$$U_{sq}(r) = \begin{cases} \infty & r < d \\ \epsilon & \sigma \le r < 1.2d \\ 0 & r \ge 1.2d \end{cases} \tag{14}$$

Figure 7b demonstrates the variation of the degree of ionization

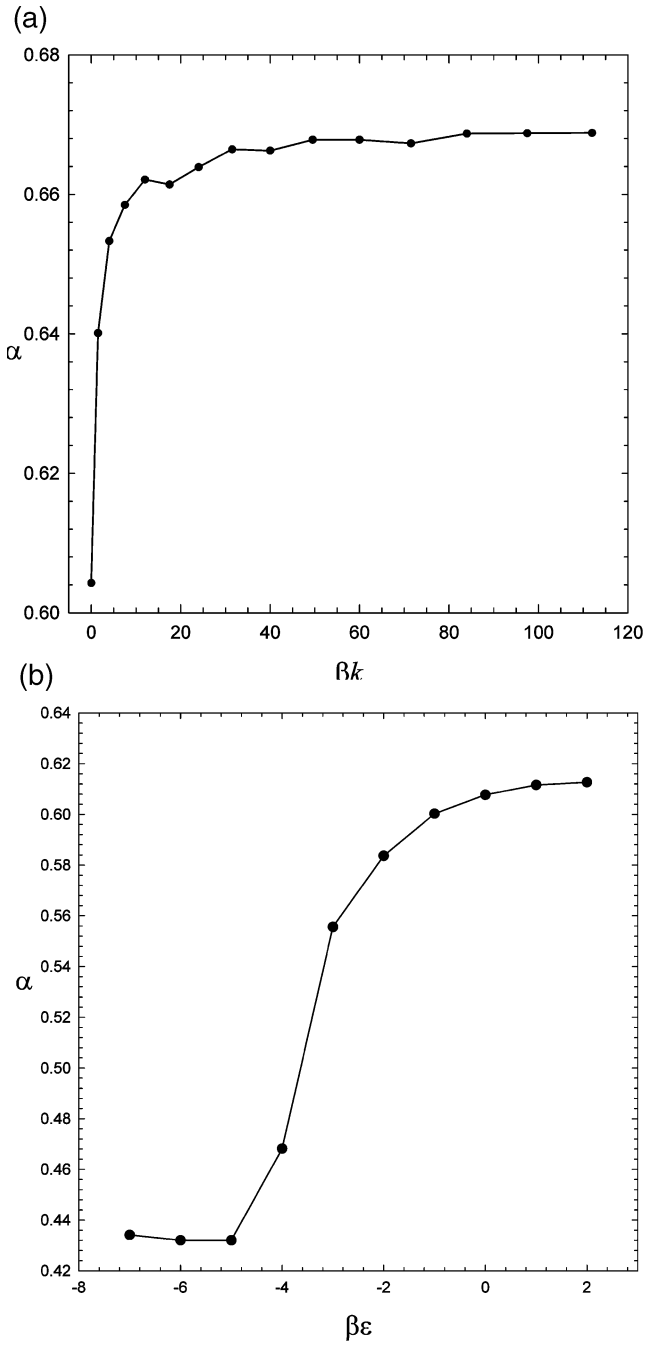

Figure 7. (a) Variation of the degree of ionization with the bending modulus βk for $N = 60$ and $\lambda = 2.50$ e/nm. (b) Variation of the degree of ionization with the solvent quality $\beta\kappa$ for $N = 60$ and $\lambda = 2.50$ e/nm.

with the solvent quality $\beta\epsilon$. Note that $\epsilon = 0$ corresponds to the hard-sphere interaction. As $\beta\epsilon$ declines, the monomer−monomer attraction results in the decrease in the polyelectrolyte size. When the inter-monomer attraction overwhelms the electrostatic repulsion, the poor solvent condition leads to a compact globule. Evidently, α declines with decreasing $\beta\epsilon$ and reaches a constant. That is, the extent of counterion condensation depends on the polymer conformation and is more significant for a compact polymer than for a flexible polyelectrolyte. Again, the characteristic size of the former is smaller than that of the latter and favors the Coulomb attraction.

F. Chain Length *N*. In a dilute, salt-free polyelectrolyte solution, both the polymer conformation and the degree of ionization may change by varying the chain length. For a single,

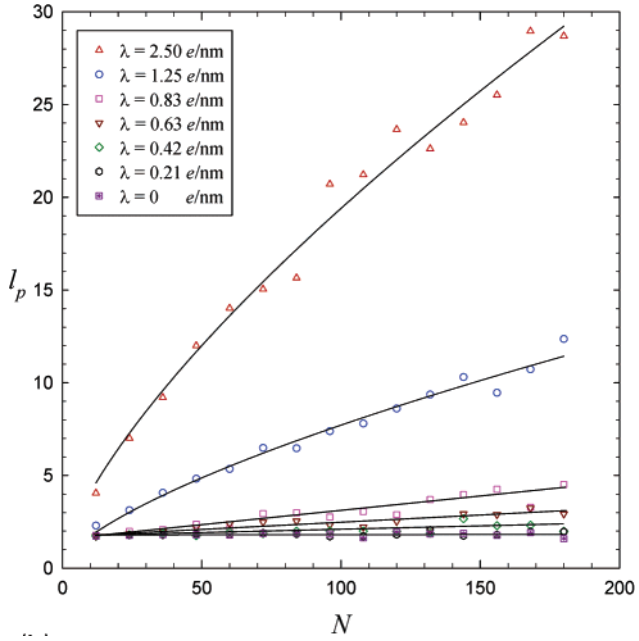

Figure 8. Variation of the persistent length with the chain length for various line charge densities. The solid lines are drawn to guide the eyes.

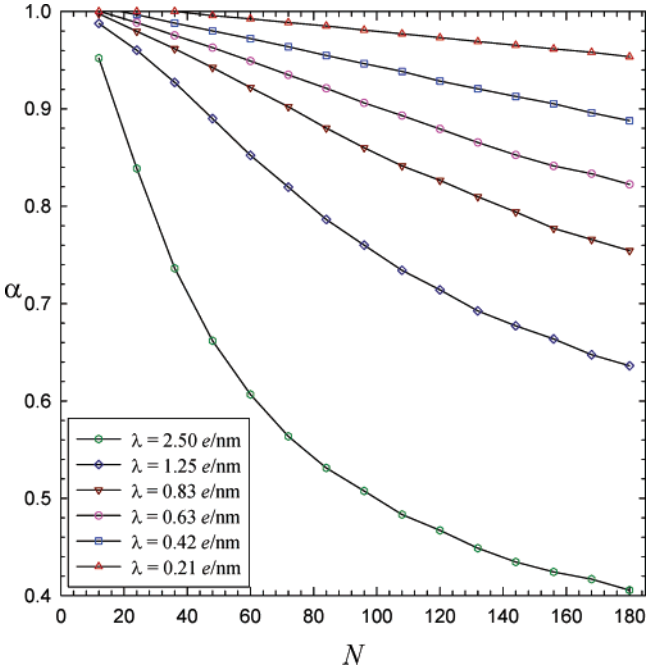

Figure 9. Variation of the degree of ionization with the chain length for various line charge densities. The solid lines are drawn to guide the eyes.

infinitely long charged polymer, the classical Odijk,[32] Skolnick and Fixman[33] (OSF) theory describes that the persistent length is a sum of intrinsic and electrostatic contributions, $l_p = l_0 + l_e$. By performing a perturbation calculation on a slightly bent, rigid charged rod using the Debye−Hückel approximation, the OSF model obtains the electrostatic persistent length[32]

$$l_e = \frac{(\lambda/e)^2 l_B}{12\kappa^2}\left[3 - \frac{8}{y} + e^{-y}\left(y + 5 + \frac{8}{y}\right)\right] \qquad (15)$$

where κ^{-1} denotes the Debye length and $y = \kappa L$ with L the contour length of the chain. The OSF expression indicates that l_e declines with increasing L and κ^2 (proportional to the concentration of added salt). However, our simulation results for the dilute, salt-free flexible polyelectrolyte solution show an opposite trend. As shown in Figure 8, the persistent length grows with increasing chain length. The increment is very significant for high line charge density, i.e., $\lambda \approx 0.83$ e/nm. This consequence reveals that the parameter range in our simulations is different from the regime applicable by the OSF theory. Note that the definition of the persistent length in eq 9 indicates that l_p is proportional to the chain length if the polymer possesses a rodlike conformation. Since $\kappa^{-1} \approx R_g$ in the cases we studied, the screening effect on the Coulomb repulsions among monomers for a flexible polyelectrolyte with finite length is insignificant. Thus, an increase in N for a high enough λ enhances electrostatic repulsions and results in the formation of a rodlike polymer. In fact, for $N = 180$ and $\lambda = 2.50$ e/nm, we have $R_g \approx 44d$, which is comparable to both the radius of gyration associated with a rod with $L = Nd$ and the persistent length $l_p \approx 30d$.

Although Muthukumar et al.[4] found the degree of ionization to be essentially independent of chain length by Langevin dynamics simulation, Winkler et al.[2] observed that α decreased with increasing N by molecular dynamic simulation. In both studies, the extent of counterion condensation was defined as the fraction of ions within an arbitrarily chosen distance perpendicular to the chain backbone. In the present investigation, we clearly find that the degree of ionization based on eq 6 varies with the chain length. Figure 9 shows that, as N grows at a given line charge density, α declines. The larger the line charge density, the more significant the decrease of the degree of ionization. When the chain length or the line charge density is increased, both the characteristic size ($\propto N^{\nu(\lambda)}$) and the intrinsic charge ($\propto \lambda N$) rises. However, the increment of the latter is faster than the former and therefore leads to an enhancement of the electrostatic attraction (counterion condensation).

G. Simple Model: Two-Phase Approximation. Counterion condensation is an essential feature of polyelectrolyte and can be understood by the competition between translational entropy and electrostatic interactions. A simple qualitative explanation for our simulation results can be provided by using the two-phase approximation.[34] One can treat the condensed and free counterions as two phases and assume that the phases are in equilibrium. The chemical potential of the free counterion is dominated by the translational entropy

$$\mu_f \simeq k_B T \ln \phi$$

where ϕ is the volume fraction of the free counterions, $\phi \approx (N_p\alpha)d^3/8R^3 \propto c_p$. The chemical potential of the condensed counterion is the Coulombic binding energy between the free counterion and the polyelectrolyte

$$\mu_c \simeq -k_B T (N_p\alpha) z_c \frac{l_B}{R_g}$$

By equating the chemical potential, one obtains

$$\alpha = -\frac{1}{N_p z_c}\left(\frac{R_g}{l_B}\right) \ln \phi \qquad (16)$$

Note that the function $\ln \phi$ varies gradually with ϕ. With $R_g = bN^\nu$ and $N_p e = \lambda N d$, the degree of ionization is given by

$$\alpha \sim \left(\frac{1}{z_c \lambda l_B d}\right)\left(\frac{1}{N^{1-\nu}}\right) \ln R \qquad (17)$$

Evidently, the degree of ionization declines with increasing line charge density (λ) and chain length (N) and with decreasing the polyelectrolyte concentration (R). If the polyelectrolyte conformation is altered by the solvent quality or bending rigidity, α rises with the characteristic size (R_g) for a given chain length. That is, the degree of ionization is highest for a finite charged rod ($d_f = 1$) and lowest for a charged globule ($d_f = 3$).

IV. Conclusion

In a salt-free solution, the phenomenon of counterion condensation around an intrinsically flexible polyelectrolyte is investigated by Monte Carlo simulations. With the polyelectrolyte fixed at the center of the spherical Wigner−Seitz cell, the characteristics of the polymer conformation such as static structure factor, radius of gyration, and persistent length can be calculated. In addition, the radial distributions of monomer and counterion and the counterion chemical potential can be obtained. Since the Debye length is larger than the polyelectrolyte size in the present study, the electrostatic interactions are essentially unscreened.

In the present spherical WS cell simulations, the effect of polyelectrolyte−polyelectrolyte is not taken into account because the neighboring polymer is absent. Our approach is justified for very dilute polyelectrolyte solutions. A rigorous justification can be made by the comparison of results between the WS cell model and the periodic boundary condition with Ewald summation. In fact, such a comparison has been made for counterion condensation on the charged particle system by Groot.[17] He concluded that the cell model provides a good description of the multibody system at low volume fraction. At high volume fraction, the results of the cell model are still qualitatively correct. This consequence reveals that long-range interactions are not significant for the counterion distribution around a structureless particle. For a flexible chain, its conformation might be perturbed by other polyelectrolytes, and thereby, the counterion distribution and the degree of ionization are altered accordingly. Nonetheless, we believe that the cell model provides at least qualitatively correct insight for the behavior associated with the effective charge of the polyelectrolyte as long as its conformation is not disturbed by the cell boundary.

The extent of counterion condensation can be expressed in terms of the degree of ionization (effective charge). Previous studies often adopt the definition of α as the fraction of counterions within an arbitrarily chosen distance perpendicular to the chain backbone. However, such a two-state definition does not relate to experimental measurements. To enable direct comparison with equilibrium experimental results, the charge renormalization is operationally performedon the basis of the thermodynamic properties such as chemical potential or osmotic pressure, which is uniform everywhere in the polyelectrolyte solution. Consequently, the free counterion concentration in the polyelectrolyte solution is represented by that of the salt solution with the same chemical potential.

The influences of polyelectrolyte concentration and properties such as chain length, bending rigidity, solvent quality, and line charge density on the degree of ionization are examined. Our simulation shows that α rises as the polymer concentration decreases. This behavior is opposite that calculated from the infinitely long charged rod model, which is often used to study counterion condensation. We also find that the degree of ionization decreases with an increment in chain length and chain flexibility. In fact, the degree of ionization is found to decline with increasing polymer fractal dimension, which can be tuned by varying bending modulus and solvent quality. Those results can be qualitatively explained by a simple model of two-phase approximation.

The persistent length, which represents a measure of stiffness or correlation along the chain, is also evaluated on the basis of the definition of the projection length. According to the classical OSF theory based on a perturbation calculation on the slightly bent rod, the electrostatic persistent length declines with increasing salt concentration and chain length and with decreasing line charge density. Consistent with the OSF theory, our results show that l_p rises with increasing line charge density. When the line charge density is high enough, however, the electrostatic persistent length also grows significantly with increasing chain length. In fact, l_p is proportional to the chain length if the polymer is represented by a rigid rod. This consequence differs from the classical OSF theory and indicates the invalidity of the OSF theory in salt-free polyelectrolyte solutions owing to the unscreened electrostatic interaction.

Acknowledgment. This research is supported by National Council of Science of Taiwan under grant no. NSC 93-2214-E-008-001. Computing time provided by the National Center for High-Performance Computing of Taiwan is gratefully acknowledged.

References and Notes

(1) Anderson, C. F.; Record, M. T., Jr. *Annu. Rev. Biophys. Biophys. Chem.* **1990**, *19*, 423. Bacquet, R.; Rossky, P. *J. Phys. Chem.* **1984**, *88*, 2660. Bratko, D.; Dolar, D. *J. Chem. Phys.* **1984**, *80*, 5782. Gordon, H. L.; Valleau J. P. *Mol. Sim.* **1995**, *14*, 361.

(2) Winkler, R. G.; Gold, M.; Reineker, P. *Phys. Rev. Lett*. **1998**, *80*, 3731. Brilliantov, N. V.; Kuznetsov, D. V.; Klein, R. *Phys. Rev. Lett*. **1998**, *81*, 1433.

(3) Deserno, M.; Holm, C.; May, S. *Macromolecules* **2000**, *33*, 199.

(4) Liu, S.; Muthukumar, M. *J. Chem. Phys.* **2002**, *116*, 9975.

(5) Liao, Q.; Dobrynin, A. V.; Rubinstein, M. *Macromolecules* **2003**, *36*, 3399.

(6) González-Mozuelos, P.; Olvera de la Cruz, M. *J. Chem. Phys*. **1995**, *103*, 3145.

(7) Roberts, J. M.; O'Dea, J. J.; Osteryoung, J. G. *Anal. Chem.* **1998**, *70*, 3667.

(8) Abuin, E. B.; Lissi, E. A.; Núñez, R.; Olea, A. *Langmuir* **1989**, *5*, 753.

(9) Hsiao, C. C.; Wang, T.-Y.; Tsao, H.-K. *J. Chem. Phys*. **2005**, *122*, 144702.

(10) Void, R. D.; Void, M. J. *Colloid and Interface Chemistry*; Addison-Wesley: Reading, 1983.

(11) Manning, G. S. *J. Chem. Phys*. **1969**, *51*, 924.

(12) Ossawa, F. *Polyelectrolytes*; Dekker: New York, 1971.

(13) Muthukumar, M. *J. Chem. Phys*. **2004**, *120*, 9343.

(14) Hsin, W. L.; Wang, T.-Y.; Sheng Y.-J.; Tsao, H.-K. *J. Chem. Phys.* **2004**, *121*, 5494.

(15) Alexander, S.; Chaikin, P. M.; Grant P.; Morales, G. J. Pincus, P. *J. Chem. Phys*. **1984**, *80*, 5776.

(16) Verwey, E. J. W.; Overbeek, J. T. G. *Theory of the Stability of Lyophobic Colloids*; Elsevier: Amsterdam, 1948.

(17) Groot, R. D. *J. Chem. Phys*. **1991**, *95*, 9191.

(18) Belloni, L. *Colloids Surf., A* **1998**, *140*, 227.

(19) Deserno, M.; Holm, C.; May, S. *Macromolecules* **2000**, *33*, 199.

(20) Deserno, M.; Holm, C. In *Electrostatic Effects in Soft Matter and Biophyiscs*; Kluwer Academic Publishers: Dordrecht, The Netherlands, 2001; p 27. Wennerström, H.; Jönsson, B.; Linse, P. *J. Chem. Phys.* **1982**, *76*, 4665.

(21) Sheng, Y.-J.; Jiang, S.; Tsao, H.-K. *Macromolecules* **2002**, *35*, 7865. Sheng, Y.-J.; Chen, J. Z.-Y.; Tsao, H.-K. *Macromolecules* **2002**, *35*, 9624. Sheng, Y.-J.; Hsu P.-H.; Chen, J. Z.-Y.; Tsao, H.-K. *Macromolecules* **2004**, *37*, 9257.

(22) Mel'nikov, S. M.; Khan, M. O.; Lindman, B.; Jönsson, B. *J. Am. Chem. Soc.* **1999**, *121*, 1130.

(23) Sheng, Y.-J.; Lin, H.-J.; Chen, J. Z. Y.; Tsao, H.-K. *J. Chem. Phys.* **2003**, *118*, 851. Tsao, H.-K.; Chen, J. Z. Y.; Sheng, Y.-J. *Macromolecules* **2003**, *36*, 5863.

(24) Frenkel, D.; Smit, B. *Understanding Molecular Simulation*; Academic: New York, 1996.
(25) Ho, C.-H.; Tsao, H.-K.; Sheng, Y.-J. *J. Chem. Phys.* **2003**, *119*, 2369. Hsin, W. L.; Sheng, Y.-J.; Lin, S.-Y.; Tsao, H.-K. *Phys. Rev E* **2004**, *69*, 031605.
(26) Deshkovski, A.; Obukhov, S.; Rubinstein, M. *Phys. Rev. Lett.* **2001**, *86*, 2341.
(27) Dobrynin, A. V.; Colby, R. H.; Rubinstein, M. *Macromolecules* **1995**, *28*, 1859.
(28) Ullner, M.; Woodward, C. E. *Macromolecules* **2002**, *35*, 1437.
(29) Liao, Q.; Dobrynin, A. V.; Rubinstein, M. *Macromolecules* **2003**, *36*, 3399.
(30) Sheng, Y.-J.; Lin, H.-J.; Chen, J. Z. Y.; Tsao, H.-K. *Macromolecules* **2004**, *37*, 9631.
(31) Chen, J. Z. Y.; Tsao, H.-K.; Sheng, Y.-J. *Europhys. Lett.* **2004**, *65*, 407.
(32) Odijk, T. *J. Polym. Sci., Polym. Phys. Ed.* **1977**, *15*, 477.
(33) Skolnick, J.; Fixman, M. *Macromolecules* **1977**, *10*, 944.
(34) Heilman-Miller, S. L.; Thirumalai, D.; Woodson, S. A. *J. Mol. Biol.* **2001**, *306*, 1157.